ChemPubSoc Europe

DOI: 10.1002/ejic.201801234

EurJIC European Journal of Inorganic Chemistry

Full Paper

Phosphorus Heterocycles | *Very Important Paper* | SPECIAL ISSUE

VIP

Re^{I} Complexes of Pyridylphosphinines and 2,2′-Bipyridine Derivatives: A Comparison

Antonia Loibl,[a] Manuela Weber,[a] Martin Lutz,[b] and Christian Müller*[a]

Dedicated to Professor Koop Lammertsma on the occasion of his 70th birthday

Abstract: The coordination chemistry of 2-(2′-pyridyl)-4,6-diarylphosphinines towards Re^{I} has been investigated and compared to the structurally analogous 2,2′-bipyridine derivatives. The different steric properties of the chelating pyridylphosphinines with respect to substituted bipyridines lead to considerable differences in the structures of the mononuclear $[(P^{\wedge}N)Re(CO)_3X]$ and $[(N^{\wedge}N)Re(CO)_3X]$ (X = Cl, Br) complexes, both in the solid state and in solution. The phosphinine-based coordination compounds are highly sensitive towards nucleophilic attack and react reversibly with water at the P=C double bond.

Introduction

2,2′-Bipyridine derivatives are among the most widely studied nitrogen-based ligands in coordination chemistry. Metal complexes containing such chelates have found a multitude of interesting applications, especially as photosensitizers in solar cells, light harvesting antennas and homogeneous catalysts, including photo- and electrochemical reactions.[1] The replacement of a pyridine unit by a π-accepting, aromatic phosphinine[2] heterocycle leads to 2-(2′-pyridyl)phosphinine, a semi equivalent of 2,2′-bipyridine (Figure 1).

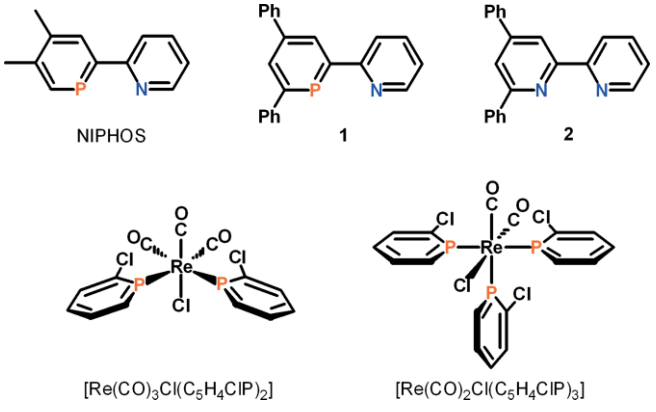

Figure 1. NIPHOS in comparison to **1** and **2**, and phosphinine complexes of Re^{I} reported in literature.

This P,N-hybrid contains a low-coordinate "soft" phosphorus atom and a "hard" nitrogen donor and has first been described by Mathey et al. in 1982 with the synthesis of 2-(2′-pyridyl)-4,5-dimethylphosphinine (NIPHOS).[3] However, only a few studies were devoted to its coordination chemistry at that time.[4] In 2007, we have demonstrated that 2-(2′-pyridyl)-4,6-diphenylphosphinine **1** (Figure 1) is readily available from the corresponding pyridyl-functionalized pyrylium salt **pypy-BF_4** and $P(SiMe_3)_3$ (Scheme 1).[5] Interestingly, this synthetic route offers at the same time access to the N,N analogue 2-(2′-pyridyl)-4,6-diphenylpyridine **2**, which makes a direct comparison of these structurally related heterocycles possible.[6]

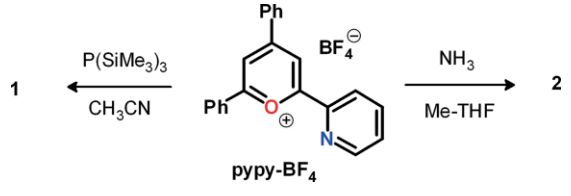

Scheme 1. Synthesis of **1** and **2**, starting from pyridyl-functionalized pyrylium salt **pypy-BF_4**.

It turned out that **1** is kinetically much more stable than NIPHOS and, consequently, its coordination chemistry has been exploited by us to quite some extend during the last decade.[7] Surprisingly, we noticed that only two phosphinine complexes of Re^{I} have been reported in literature so far: $[Re(CO)_3Cl(C_5H_4ClP)_2]$ and $[Re(CO)_2Cl(C_5H_4ClP)_3]$ (Figure 1).[8] As coordination compounds of the type $[Re(bpy)(CO)_3Cl]$ have attracted considerable interest in the field of photochemical and electrochemical reduction of CO_2, we now started to investigate the synthesis and characterization of Re^{I} complexes containing the chelating P,N-hybrid ligand **1**.[9] Our results are compared in detail to the structural N,N analogue 2-(2′-pyridyl)-4,6-diphenylpyridine **2**.

[a] *Institut für Chemie und Biochemie, Freie Universität Berlin, Fabeckstr. 34/36, 14195 Berlin, Germany*
E-mail: c.mueller@fu-berlin.de
www.bcp.fu-berlin.de/ak-mueller
[b] *Bijvoet Center for Biomolecular Research, Crystal and Structural Chemistry, Utrecht University, Padualaan 8, 3584 CH Utrecht, The Netherlands*
Supporting information and ORCID(s) from the author(s) for this article are available on the WWW under https://doi.org/10.1002/ejic.201801234.

Results and Discussion

As we have demonstrated before, the pyrylium salt route depicted in Scheme 1 is a modular synthetic procedure and allows the introduction of different substituents in the aryl groups in 4- and 6-position of the heterocycle. In the context of investigating substituent effects on electronic properties of phosphinines, we have recently synthesized a series of derivatives of **1** and **2** via the corresponding substituted, highly fluorescent pyrylium salts.[10,11] It turned out, that a fluorine atom in *para*-position of the 4-aryl ring has only a marginal effect on the energetic position of the frontier orbitals of the pyridyl-functionalized heterocycles. Nevertheless, we chose for using **pypy-F-BF$_4$** as a starting material for this study because the F-substituent often influences drastically the crystallization behavior and solubility of pyrylium salts, 2,4,6-triarylphosphinines as well as the corresponding transition metal complexes. As an example, the molecular structure of **pypy-F-BF$_4$** in the crystal is depicted in Figure 2, along with selected bond lengths and distances.[11] It is obvious that the central pyrylium-ring is almost co-planar with the pyridyl-ring in 2- and the aryl-rings in 4- and 6-position. The bond lengths C(1)–C(11) [1.462(2) Å], C(3)–C(17) [1.467(3) Å] and C(5)–C(6) [1.475(3) Å] are considerably shorter than a carbon–carbon single bond, indicating delocalization of the π-systems over the aromatic rings.

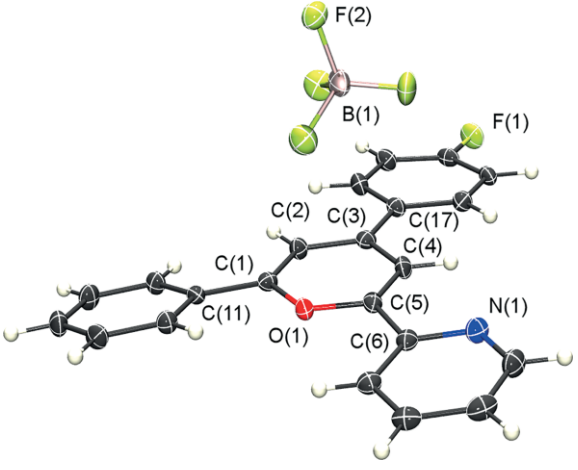

Figure 2. Molecular structure of **pypy-F-BF$_4$** in the crystal. Displacement ellipsoids are shown at the 50 % probability level. Selected bond lengths [Å]: O(1)–C(1): 1.351(2); O(1)–C(6): 1.348(2); C(1)–C(11): 1.462(2); C(5)–C(6): 1.475(3); C(3)–C(17): 1.467(3). Reproduced from ref.[11] with permission of The Royal Society of Chemistry.

Pyrylium salts **pypy-BF$_4$** and **pypy-F-BF$_4$** were converted into the corresponding pyridylphosphinines and 2,2′-bipyridine derivatives **1**, **1-F**, **2** and **2-F**, as recently described by us (Scheme 1).[10,11] Heating [Re(CO)$_5$X] (X = Cl, Br) in a solution of the pyridylphosphinine **1** and **1-F** gives the corresponding Re^I complexes of the type [(P^N)Re(CO)$_3$X], according to Scheme 2. While the reaction proceeds faster in DCM and THF, toluene was chosen to simplify workup. The complexes [(P^N)Re(CO)$_3$Cl] (**3**, **3-F**) and [(P^N)Re(CO)$_3$Br] (**4**, **4-F**) were obtained as bright yellow, crystalline and water-sensitive solids in 68–75 % isolated yield (racemic mixtures). All Re^I complexes showed a good solubility in dichloromethane and tetrahydrofuran. While transition metal complexes of 2,4,6-triarylphosphinines usually show chemical shifts between δ = 150–170 ppm in the $^{31}P\{^1H\}$ NMR spectrum, the $^{31}P\{^1H\}$ coordination chemical shift difference $\Delta\delta$ is rather small and in the order of 1.5 ppm for the new Re^I complexes. As an example, the fluorine-substituted pyridylphosphinine **1-F** shows a resonance at δ = 186.7 ppm in the $^{31}P\{^1H\}$ NMR spectrum, while a signal at δ = 188.1 ppm is observed for the respective Re^I chloride complex **3-F**. Following the course of the complexation reaction by means of $^{31}P\{^1H\}$ NMR spectroscopy further reveals, that the ligand exchange reaction (2 CO vs. P,N) proceeds without the appearance of the mono-P-coordinated species [(N∩P)Re(CO)$_4$X], as observed during the synthesis of the closely related tungsten(0) hexacarbonyl complexes of the type [(P^N)W(CO)$_4$].[7h,11]

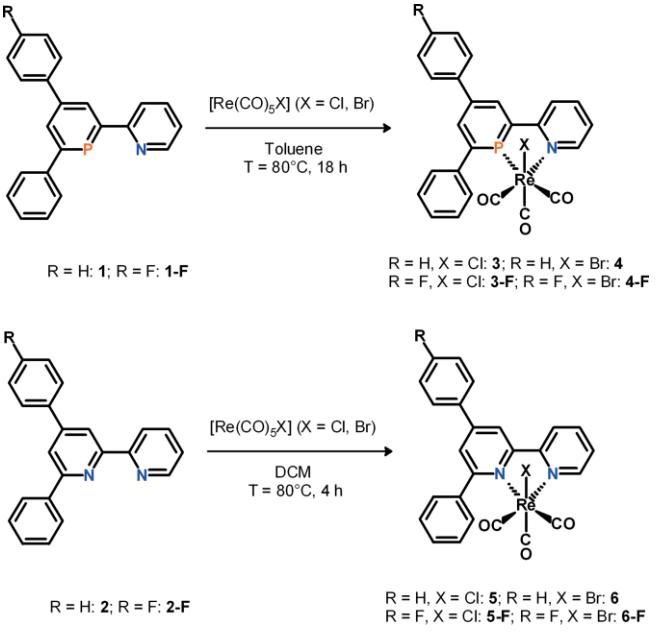

Scheme 2. Synthesis of Re^I complexes starting from **1**, **1-F**, **2** and **2-F**.

For the synthesis of [(bipy)Re(CO)$_3$X] complexes, a number of various synthetic procedures can be found in literature.[12] We noticed, that if bipyridine derivatives **2** and **2-F** were dissolved in DCM and added to [Re(CO)$_5$X] (X = Cl, Br) in a J. Young NMR tube, yellow crystals of the bipyridine-based Re^I complexes **5**, **5-F**, **6** and **6-F** are formed after a few minutes at *T* = 80 °C (Scheme 2). The products can easily be filtered off from the reaction mixture and dried in vacuo to give bright yellow, crystalline solids in 67–82 % isolated yield. In contrast to the phosphinine-based coordination compounds, all bipyridine-based complexes are hardly soluble in DCM, THF, benzene, acetone, acetonitrile or methanol. Moreover, **5**, **5-F**, **6** and **6-F** are stable towards air and moisture and can be heated in DMSO until boiling temperature (*T* = 189 °C) without showing any signs of decomposition.

Single crystals of **4** and **6**, suitable for X-ray crystallography, were obtained by slow recrystallization of the complexes from toluene and dichloromethane, respectively. The molecular structure in the solid state of both compounds is depicted in

Figure 3a/b along with selected bond lengths and angles. As expected from the thermal method of synthesis, both **4** and **6** show the presence of the *fac*-isomer (*fac* in relation to the three carbonyl ligands), with the P,N-hybrid ligand and the 2,2′-bipyridine derivative acting as a bidentate chelate. For [(bipy)Re(CO)$_3$Cl] the transformation into the *mer*-conformation by irradiation with UV light under a CO atmosphere has been reported.[13] **4** and **6** show a distorted octahedral arrangement of the ligands around the metal center. While the Re^{I} atom is located in the ideal coordination axis of the pyridyl moiety, it is significantly shifted from the expected position at the phosphorus donor towards the N(1) atom. This non-directional coordination has been observed for related transition metal complexes of pyridyl-functionalized phosphinines before and is facilitated by the larger, more diffuse and less directional lone pair of the phosphorus atom in comparison to the one of the nitrogen atom, while maintaining at the same time the chelating coordination.[7]

The crystallographic characterization of **4** and **6** further reveals, that the P^N and N^N-heterocycles are only slightly twisted with respect to one another [torsion angle P(1)–C(5)–C(6)–N(1) = 9.5(2)° and N(1)–C(5)–C(6)–N(2) = –6.6(3)°]. The intercyclic C(5)–C(6) bond length in **6** is with 1.481(3) Å only marginally shorter than the value found for free 2,2′-bipyridine [1.490(3) Å], while the corresponding data for **1** have not been reported in literature so far.[14] The P–C bonds of 1.7156(19) Å and 1.7194(18) Å, as well as the C–C bonds of 1.388(3)–1.401(3) Å of the phosphorus heterocycle are in the expected range for transition metal phosphinine complexes.[7] The most striking difference between **4** and **6** is, however, the impact of the different heteroatoms on the molecular structure of the Re^{I} complexes in the solid state. Due to the longer P(1)–C(1) and

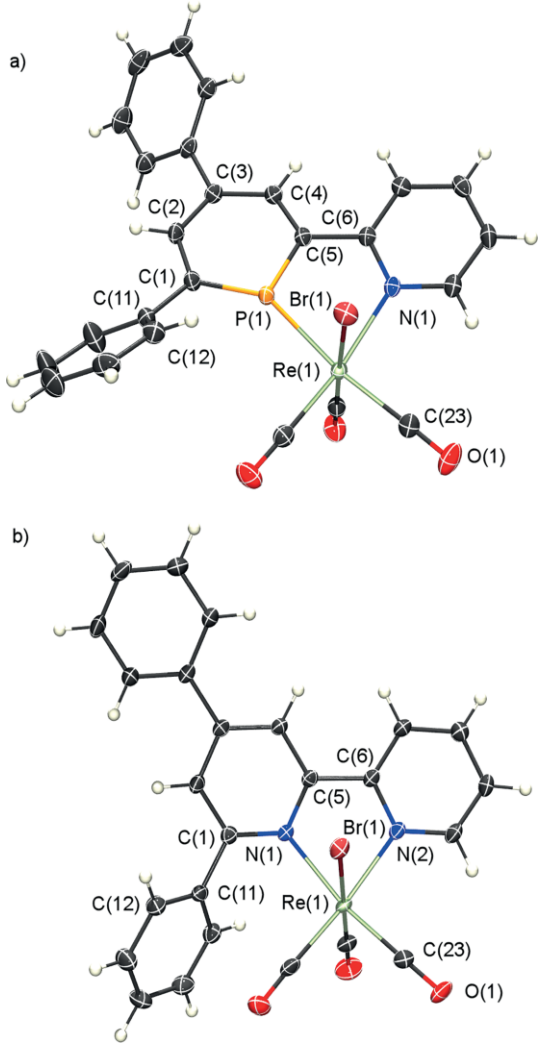

Figure 3. Molecular structures of **4** (a) and **6** (b) in the crystal. Displacement ellipsoids are shown at the 50 % probability level. Selected bond lengths [Å] and angles [°]: **4**: P(1)–C(1): 1.7156(19); P(1)–C(5): 1.7194(18); C(1)–C(2): 1.395(3); C(2)–C(3): 1.397(3); C(3)–C(4): 1.401(3); C(4)–C(5): 1.388(3); C(5)–C(6): 1.476(3); C(1)–C(11): 1.481(3); P(1)–Re(1): 2.3657(5); N(1)–Re(1): 2.2415(15). P(1)–Re(1)–N(1): 75.58(4); P(1)–C(1)–C(11)–C(12): 40.8(2). **6**: C(5)–C(6): 1.481(3); N(1)–Re(1): 2.2199(16); N(2)–Re(1): 2.1672(17). N(1)–Re(1)–N(2): 74.83(6); N(1)–C(1)–C(11)–C(12): 125.5(2).

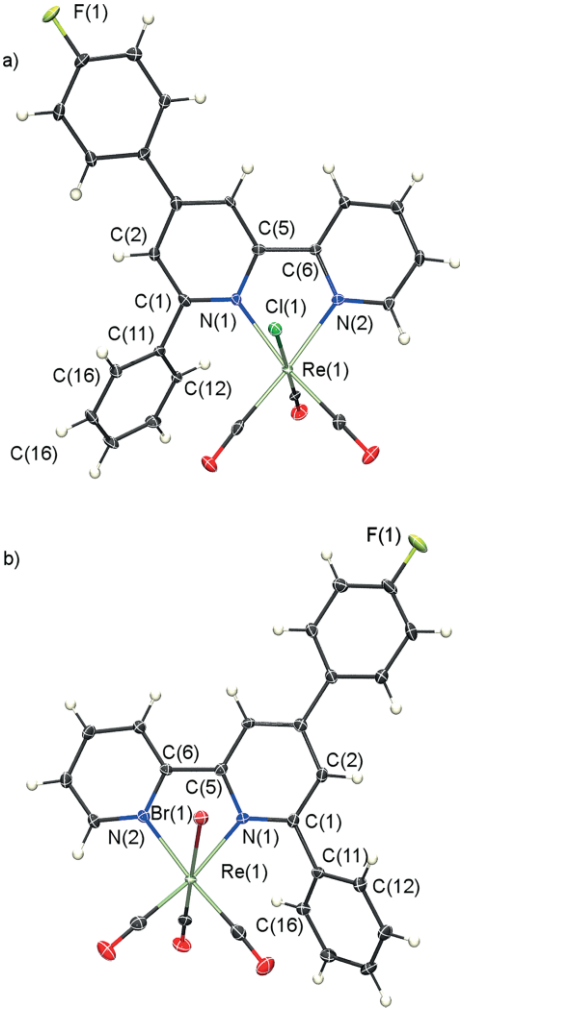

Figure 4. Molecular structures of **5-F** (a) and **6-F** (b) in the crystal. Displacement ellipsoids are shown at the 50 % probability level. Solvent molecules are omitted for clarity. Selected bond lengths [Å] and angles [°]: **5-F**: 5-F: C(5)–C(6): 1.471(5); N(1)–Re(1): 2.216(3); N(2)–Re(2): 2.171(3). N(1)–Re(1)–N(2): 74.31(11); N(1)–C(1)–C(11)–C(12): –53.0(4). **6-F**: C(5)–C(6): 1.477(4); N(1)–Re(1): 2.216(2); N(2)–Re(1): 2.171(2). N(1)–Re(1)–N(2): 74.46(8); N(1)–C(1)–C(11)–C(16): 52.8(3).

P(1)–Re(1) bond lengths in **4** compared to the N(1)–C(1) and N(1)–Re(1) bond length in **6**, the phenyl group in 6-position of the central heterocycle is considerably shifted away from the coordination site (Figure 3a). In contrast, the phenyl-substituent in α-position of the N(1)-pyridine ring in **2** is much closer to the [Re(CO)$_3$Br] fragment (Figure 3b). The same situation is found for the crystallographically characterized complexes **5-F** and **6-F**, containing the fluorine-substituted 2,2′-bipyridine derivative **2-F** as ligand (Figure 4a/b).

The steric repulsion between the α-phenyl-ring and the CO ligand *trans* to N(2) even causes a significant elongation of the N(1)–Re(1) bond, compared to the N(2)–Re(1) bond [2.2199(16) Å (**6**); 2.216(3) Å (**5-F**); 2.216(2) Å (**6-F**) vs. 2.1672(17) Å] (**6**); 2.171(3) Å (**5-F**); 2.171(2) Å (**6-F**). This situation also leads to rather different torsion angles of P(1)–C(1)–C(11)–C(12) = 40.8(2)° and N(1)–C(1)–C(11)–C(12/16) = 125.5(2)° (**6**), –53.0(4)° (**5-F**) and 52.8(3)° (**6-F**). Interestingly, this enforced orientation of the α-aryl-group in the coordination compounds has a direct effect on the structure of **4**, **6**, **5-F** and **6-F** in solution (vide infra).

Upon coordination of a phosphinine to a transition metal atom, a widening of the internal C–P–C angle from approximately 100° to higher values is usually observed.[15] It has been found that the C-P–C angle can be used as an indicator for the kinetic stability against attack of a nucleophile to the phosphorus atom of phosphinine-based complexes. In this respect, a wider angle reflects a larger disruption of aromaticity in the heterocycle, as the lone pair requires a higher *p*-character for coordination. Coordination compounds of phosphinines with C-P–C angles below 106° are usually stable towards water and alcohols, as was confirmed for several pyridylphosphinine complexes of W^0.[7h,11] For compound **4**, a C-P–C angle of 106.3° is found and indeed, this Re^I complex is sensitive towards reaction with H_2O at the P=C double bond (vide infra).

A closer look at the ^{1}H NMR spectra of the 2,2′-bipyridine-based Re^I carbonyl complexes **5**, **5-F**, **6** and **6-F** reveals the presence of broad resonances between δ = 7.5–7.8 ppm. As an example, the aromatic region of the ^{1}H NMR spectrum of **6-F** in [D$_6$]DMSO is depicted in Figure 5.

These broad resonances are absent in the ^{1}H NMR spectra of the corresponding phosphinine complexes **3**, **3-F**, **4** and **4-F**. Depending on the overlap with other signals, the integrals add up to five protons and can be assigned to the protons of the 6-phenyl ring of the central heterocycles, as determined by means of 2D NMR spectroscopy. Apparently, rotation of the 6-phenyl ring around the C(1)–C(11) bond in these coordination compounds is slow on the NMR timescale, leading to the observed broadening of the respective resonances (Figure 3, Figure 4, and Figure 6). This observation is in line with our findings concerning the pronounced differences in the molecular structures between [(P^N)Re(CO)$_3$X] and [(N^N)Re(CO)$_3$Br] complexes in the solid state (vide supra). We anticipate that the close proximity of the 6-aryl-group to the [Re(CO)$_3$X] fragment, which is absent in the phosphinine-based complexes due to the considerably longer P–C bond length, causes a hindered rotation around the C(1)–C(11) bond in the Re^I-bipyridine compounds.

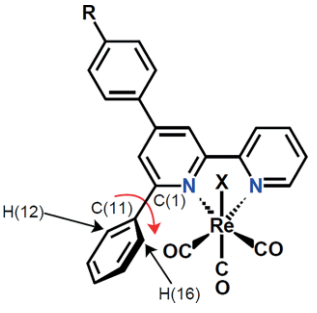

Figure 6. Hindered rotation of the 6-phenyl ring around the C(1)–C(11) bond in [(N^N)Re(CO)$_3$X] complexes due to an interaction of the phenyl group with the [Re(CO)$_3$X] fragment.

In order to evaluate the respective kinetic data, we carried out temperature dependent NMR experiments. Heating a sample of **6-F** in [D$_8$]THF leads to a faster rotation of the 6-phenyl ring, making protons H^{12}/H^{16} indistinguishable on the timescale of a NMR experiment. Upon cooling down the sample, on the other hand, the rotation of the 6-phenyl ring slows down, leading to a separation of the respective resonances (Figure 6 and Figure 7).

However, in the temperature dependent ^{1}H NMR spectra of the fluorine-substituted complex [(N^N)Re(CO)$_3$X] (**6-F**), only one of the expected two sets of proton pairs was observed to split into two resonances at low temperature, (blue asterisk). Nevertheless, we could calculate a Gibbs energy of $\Delta G^{\neq}$ = 60.3 kJ/mol and a rate constant of k_{Tc} = 104.4 s^{-1} at the coalescence temperature for the rotational barrier of the 6-phenyl ring around the C(1)–C(11) bond. The second pair of protons (Figure 7, red asterisk) does not give identifiable resonances in this temperature range, also due to overlapping signals. We also carried out variable temperature NMR spectroscopy on the unsubstituted coordination compound **6**, for which a comparable rotational barrier of $\Delta G^{\neq}$ = 58.6 kJ/mol was determined.

We were further interested in evaluating the electronic properties of the P,N-ligand in comparison to the 2,2′-bipyridine derivatives via IR spectroscopy. It is well known that phosphinines

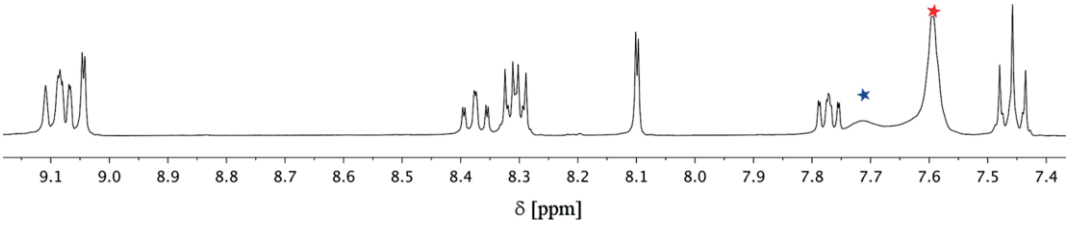

Figure 5. ^{1}H NMR spectrum of the fluorine-substituted Re^I complex **6-F** in [D$_6$]DMSO. Only the aromatic region is shown. Signals corresponding to the protons of the 6-phenyl-group are marked with a blue and a red asterisk.

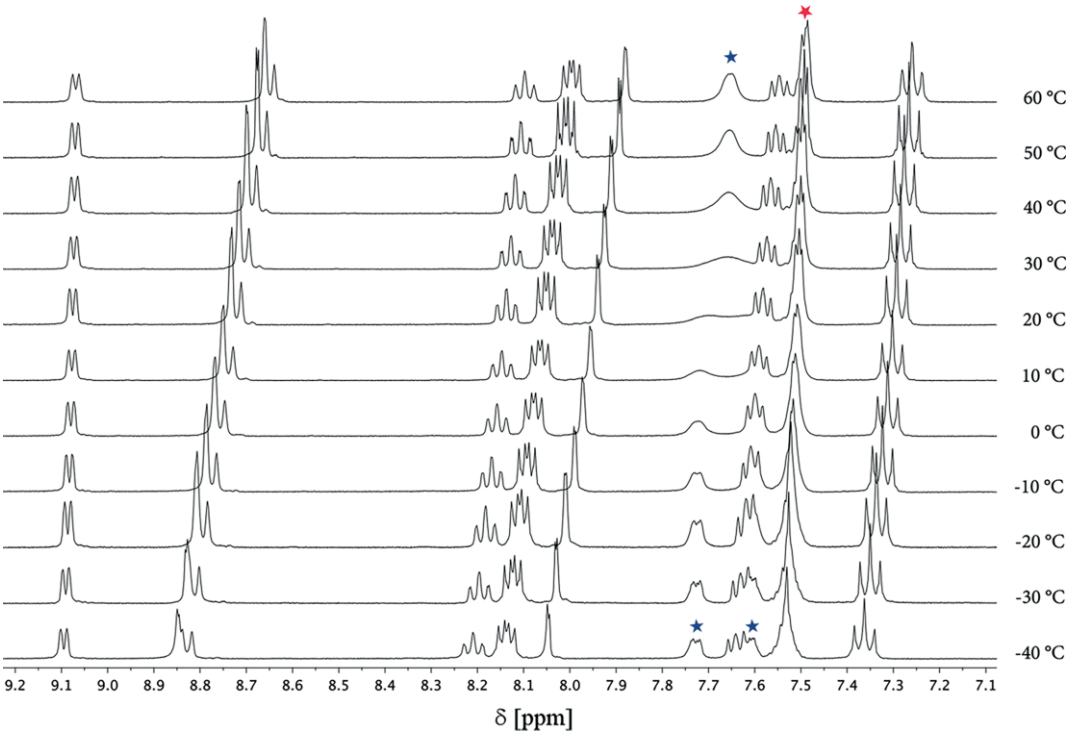

Figure 7. Temperature dependent ^{1}H NMR experiments in [D_8]THF of fluorine-substituted [N^N-Re(CO)$_3$Br] complex **6-F**. Spectra were measured in steps of 5 °C but not all spectra are shown for better clarity. Protons of the 6-phenyl ring are marked with blue and red asterisks.

possess significant π-acceptor properties, while the σ-donating ability is considered to be rather weak.[16] The net electron donor capacity of phosphinines has been evaluated before in several transition metal carbonyl complexes of phosphinines.[7h,10,11] As we have demonstrated for a series of substituted [(P^N)W(CO)$_4$] and [(N^N)W(CO)$_4$] complexes that a fluorine atom in *para*-position of the 4-aryl-ring has only a marginal effect on $\tilde{\nu}_{(CO)}$ in the corresponding IR spectra, we decided to compare only complexes **3** and **4** (P^N) with **4** and **6** (N^N).[10,11] The metal precursor [Re(CO)$_5$Cl] shows IR bands at $\tilde{\nu}_{(CO)}$ = 2155, 2046, 1983 cm^{-1}. The substitution of two strongly π-accepting carbonyl ligands by two good π-acceptor and moderately σ-donating phosphinines shifts the remaining carbonyl stretching bands significantly towards smaller wavenumbers ($\tilde{\nu}$ = 2046, 1992, 1945 cm^{-1}), as observed for the only reported phosphinine-based Re^I complex *cis*-[(L)$_2$Re(CO)$_3$Cl] (L = 2-chlorophosphinine, see Figure 1).[8] The P^N-based Re^I complexes **3** and **4** show carbonyl stretching bands at $\tilde{\nu}$ = 2029, 1948, 1937, 1905 (sh), 1880 cm^{-1} and $\tilde{\nu}$ = 2026, 1935, 1899 cm^{-1}, respectively. In contrast, the bipyridine-based compounds **5** and **6** show bands at $\tilde{\nu}$ = 2017, 1938, 1907, 1864 cm^{-1} and $\tilde{\nu}$ = 2018, 1940, 1911, 1867 cm^{-1}, respectively (Table 1). These values for the [(N^N)Re(CO)$_3$X]-type compounds **5** and **6** are very close to the ones observed for the well-investigated complex [(bipy)Re(CO)$_3$Cl].

Table 1 confirms the significantly higher CO stretching frequencies found for the P,N-based Re^I complexes, compared to the 2,2′-bipyridine-substituted derivatives. As anticipated, this phenomenon can be attributed to the higher π-accepting character of the phosphinine heterocycle with respect to the more σ-donating pyridine moiety. It should be noted here that the X-group apparently does not influence the C-O stretching bands, as only marginal differences in the IR spectroscopic data of the Re^I chloride and Re^I bromide complexes are detectable.

Table 1. Carbonyl stretching bands in the solid state FT-IR spectra of [(P^N)Re(CO)$_3$X]-type complexes **3** and **4** in comparison to [(N^N)Re(CO)$_3$X]-type complexes **5**, **6**, and **[(bipy)Re(CO)$_3$Cl]**.

	3	**4**	**5**	**6**	[(bipy)Re(CO$_3$)Cl]
	R = H X = Cl	R = H X = Br	R = H X = Cl	R = H X = Br	
$\tilde{\nu}_{(CO)}$ [cm]$^{-1}$	2029 1948 1937 1905 (sh) 1880	2026 1935 (sh) 1899 	2017 1938 1907 1864	2018 1940 1911 1867	2014 1971 1889 1859

As mentioned above, the [(P^N)Re(CO)$_3$X] complexes show a high sensitivity towards protic reagents. In fact, the facile reaction of water or alcohols with the P=C-double bond of a series of complexes containing pyridylphosphinines is known in literature. Mathey and co-worker reported first on Pd^{II} and Pt^{II} complexes of the type [(NIPHOS)MClL•ROH][PtCl$_3$L] (Figure 8).[4a] For [(P^N)MCl$_2$•CH$_3$OH] and [Cp*(P^N)MCl•H$_2$O]Cl (Pd^{II}, Pt^{II}, Ir^{III} and Rh^{III}) we could demonstrate for the first time by means of X-ray diffraction and NMR experiments, that the addition of water and alcohols to the P=C double bond proceeds exclusively either in an *syn*- (Pd, Pt), or in a *anti*-fashion (Rh, Ir) (Figure 8).[7b,7d] Moreover, all reported complexes have so far in common, that the reaction proceeds selectively at the external double bond of the P,N-hybrid ligand. Consequently, only one

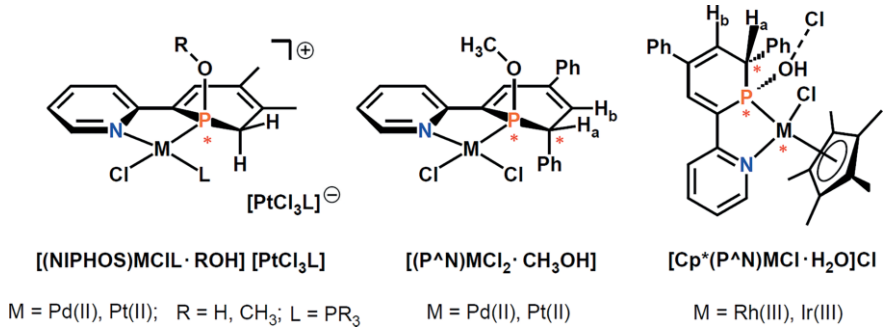

Figure 8. H_2O and CH_3OH addition products of transition metal complexes of pyridylphosphinines.

single resonance is observed in the corresponding $^{31}P\{^1H\}$ NMR spectra of these compounds. Pairs of enantiomers are formed in this reaction, when the addition of the protic reagent proceeds from the top and the bottom of the ligand plane, respectively. The starting complex of [Cp*(P^N)MCl•H_2O]Cl, [Cp*(P^N)-MCl]Cl, exists already as a racemate due to the presence of a stereogenic metal atom and the selective *anti*-addition of H_2O to the external P=C-double bond occurs only from one side of the P,N-ligand.[7d]

The high selectivity for the attack of the external P=C double bond is attributed to the electron withdrawing nature of the nitrogen atom, which decreases the nucleophilicity of the C(5) carbon atom of the internal P=C double bond.[7b] Moreover, the formation of the internal addition product is unfavoured due to geometrical constraints.[7b] The reason for the opposite *syn-anti*-selectivity remains unknown, but might be due to either a concerted or a two-step mechanism of the addition reaction.[4a] We investigated the reaction of **4** with H_2O in more detail. Surprisingly, it turned out that four new resonances at δ = 72.9, 81.2, 95.2 and 107.2 ppm in a ratio of 1:40:9:49 can be observed in the $^{31}P\{^1H\}$ NMR spectrum upon addition of degassed water to a solution of **4** in [D_2]DCM (Figure 9).

The chemical shifts of the new resonances are in agreement with the reported values for water-addition products of pyridylphosphinine complexes.[7b,7d] Even though integration of the resonances in the $^{31}P\{^1H\}$ NMR spectrum is biased by the nuclear Overhauser effect (NOE), the close structural relation between the formed species should allow the use of signal ratios for an overall picture of this reactivity study. In contrast to the observed stereoselective addition of protic reagents to the P=C double bond (vide supra), the reaction of the Re^I complex **4** with H_2O apparently proceeds rather unselectively. At this point we have to assume, that the addition of water to the external P=C double bond of **4** occurs both in *syn*- and *anti*-fashion and, additionally, also from the *re*- and the *si*-site of the complex. This would indeed lead to a mixture of four stereoisomers, as we exclude again the addition of the substrate to the internal P=C double bond. Additionally, the reaction already starts from a racemic mixture of enantiomeric complexes since the Re^I atom represents a stereogenic metal center. Therefore, the formation of a total of eight possible stereoisomers in four pairs of enantiomers have to be considered (Scheme 3). Judging from the rather different intensities of the signals, however, it has to be assumed that the formation of at least two pairs of enantiomers, corresponding to the resonances at δ = 72.9 and 95.2 *ppm*, is unfavored.

The addition of water to the Re^I complex **4** in DCM was further followed by means of $^{31}P\{^1H\}$ NMR spectroscopy (Figure 10). We noticed that the addition reaction is slow at room temperature. Even though coordination compound **4** was found to react even with traces of water left in dry solvents, the starting material is still the major resonance in the $^{31}P\{^1H\}$ NMR spectrum after approximately 10 min at room temperature. Even after one hour, part of **4** is still present in solution. Interestingly, the ratio between the four pairs of enantiomers changes with time. Thus, after one hour, a ratio 0:57:14:29 could be detected at room temperature.

Consequently, we anticipate that the water-addition to **4** is reversible, leading to an equilibrium between the eight stereoisomers in solution (Scheme 4).

This prompted us to examine the influence of the temperature on the reaction of H_2O with **4**. After addition of degassed

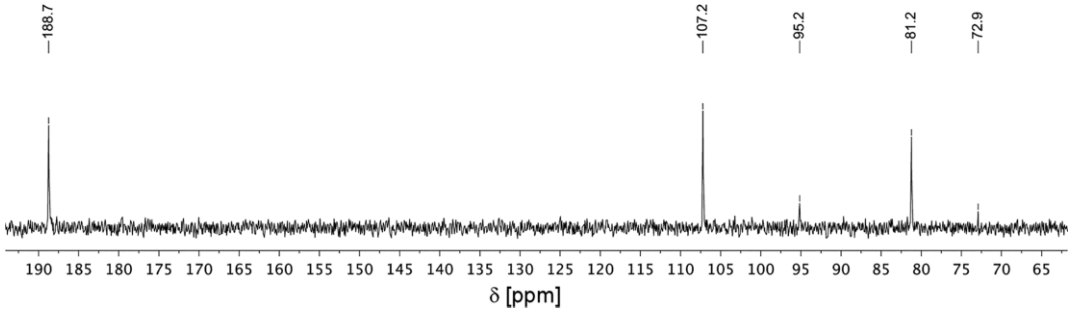

Figure 9. $^{31}P\{^1H\}$ NMR spectrum in [D_2]DCM of [(P^N)Re(CO)$_3$Br] (**4**) approximately 10 min after the addition of a drop of degassed water.

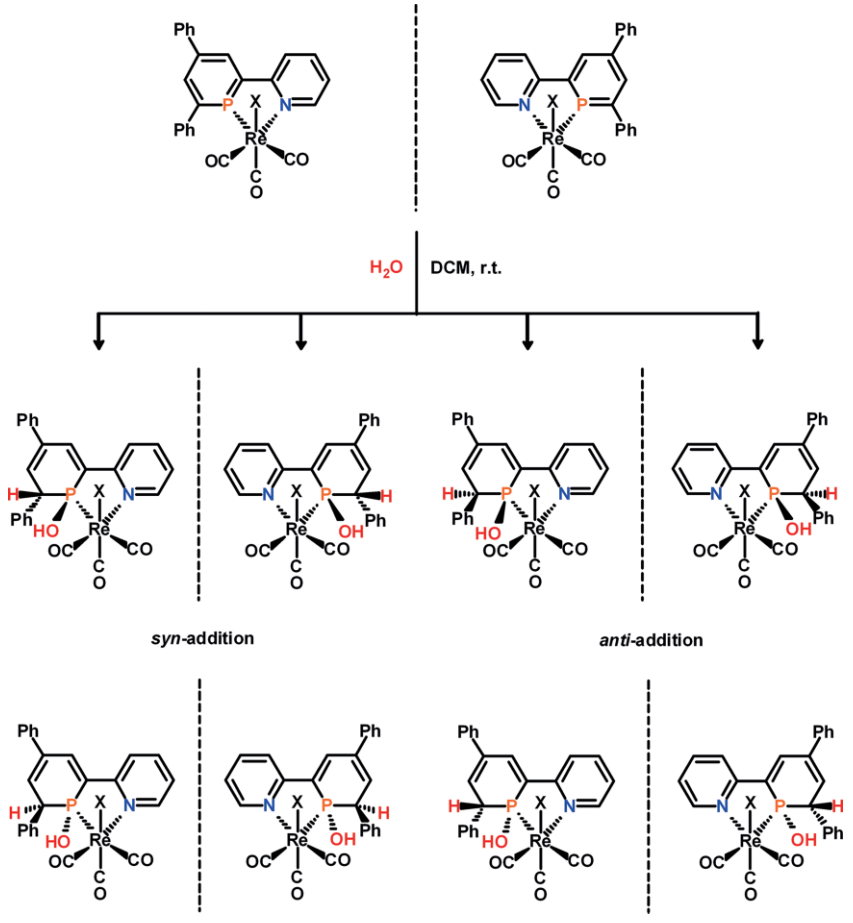

Scheme 3. Possible stereoisomers formed by reaction of **4** with water.

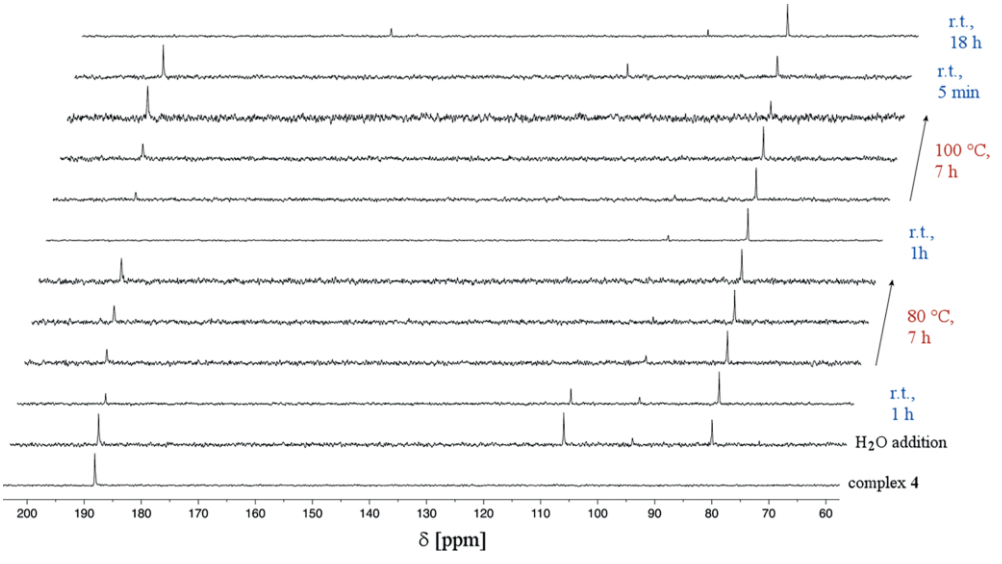

Figure 10. Time and temperature dependent $^{31}P\{^{1}H\}$ NMR experiments for the reaction of **4** with water in DCM.

water to a sample of **4** in $[D_2]$DCM and a delay of one hour at room temperature, the reaction mixture was heated to T = 80 °C, while $^{31}P\{^{1}H\}$ NMR spectra were measured in regular time intervals (Figure 10). Apparently, at higher temperatures, two resonances at δ = 72.9 and 107.2 ppm vanish immediately. Thus, these two signals can be assigned to the kinetic products of the water-addition. Interestingly, after seven hours at T = 80 °C, only two resonances remain detectable, the one of the starting material (δ = 188.7 ppm) and the one at δ = 81.2 ppm in a ratio of 45:55. Upon cooling down the sample to room

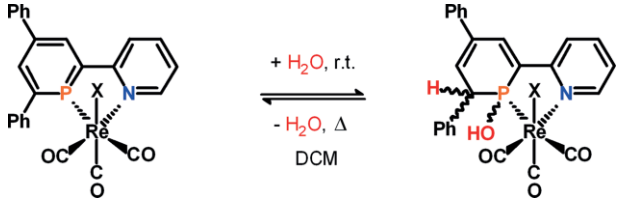

Scheme 4. Equilibrium reaction of [(P^N)Re(CO)$_3$Br] (**4**) with water.

temperature, the starting material is completely consumed and only the two thermodynamic products at δ = 81.2 and δ = 95.2 ppm can be observed exclusively after one hour at room temperature, while the species with the resonance at δ = 81.2 ppm is clearly the thermodynamically preferred complex (ratio 85:15). Upon heating the sample again to even higher temperatures, the starting material is formed again, which impressively shows that the addition of H_2O to **4** is indeed reversible. After seven hours at T = 100 °C a ratio of 75:25 between complex **4** and [(P^N)Re(CO)$_3$Br•H_2O] is reached. Upon cooling down the sample to room temperature, the equilibrium is shifted again to the side of the two thermodynamically preferred water-addition products.

These time and temperature dependent NMR experiments show an unselective but rather unusual temperature dependent reversible addition of H_2O to the [(P^N)Re(CO)$_3$Br] complex **4**. This type of reaction has so far not been observed for transition metal complexes based on phosphinines. However, the number of repetitions seems to be limited. Already after two cycles the appearance of a new signal can be detected at δ = 150.0 ppm in the $^{31}P\{^1H\}$ NMR spectrum. Leaving the reaction mixture at room temperature for several days, a multitude of resonances for unidentified decomposition products around δ = 135–155 ppm can be detected by means of $^{31}P\{^1H\}$ NMR spectroscopy.

The lack of crystallographic and NMR spectroscopic data prohibits the determination of major and minor, as well as of kinetic and thermodynamic products in this equilibrium reaction up to this point. Nevertheless, the reversible addition of water to the P=C-double bond of the phosphorus heterocycle could play an interesting role in catalytic processes, in which the transfer of protons and/or water molecules is required. This concept is currently evaluated in our laboratories.

Conclusions

In summary, we have prepared and crystallographically characterized the first Re^I-carbonyl complex containing the P,N hybrid ligand 2-(2′-pyridyl)-4,6-diarylphosphinine. This coordination compound was compared in detail with the related 2,2′-bipyridine derivative. Substantial structural differences between the two complexes were observed, which can mainly be attributed to the significantly longer P–C bond length in the phosphinine heterocycle compared to the N–C bond length in a pyridine moiety. The geometrical features of phosphinines influence particularly the alignment of the remaining phenyl group in 6-position of the central ring, which is considerably shifted away from the coordination site. As a consequence the rotation of the 6-phenyl ring around the inter-ring C–C bond is fast on the NMR timescale for complexes of the type [(P^N)Re(CO)$_3$X], while it is slow for coordination compounds of the type [(N^N)Re(CO)$_3$X], due to steric repulsion of the phenyl group with the [Re(CO)$_3$X] fragment. The corresponding rotational barriers were determined experimentally. The [(P^N)Re(CO)$_3$Br] complexes further turned out to be rather sensitive towards protic reagents. At room temperature, they react unselectively with water at the external P=C-double bond, leading to a mixture of stereoisomers. Interestingly, however, it turned out that the water-addition reaction is reversible, as demonstrated by means of variable temperature NMR spectroscopy.

Experimental Section

General Remarks: Experiments were performed under an inert argon atmosphere and were carried out using modified Schlenk techniques or in a MBraun dry box. All common chemicals were commercially available and purchased from Aldrich Chemical Co., ABCR, Alfa Aesar, Acros as well as Eurisol and were used as received. Dry or deoxygenated solvents were prepared using standard techniques or used from an MBraun MB SBS-800 solvent purification system. Tetrahydrofuran and diethyl ether were distilled under argon over potassium/benzophenone and sodium/benzophenone, respectively. The ^1H, $^{13}C\{^1H\}$, ^{19}F and $^{31}P\{^1H\}$ NMR spectra were recorded on a JEOL EXZ400 (400 MHz) or a JEOL ECX400 (400 MHz) FT spectrometer and chemical shifts are reported relative to the residual resonance of the deuterated solvents. Mass spectrometry has been performed on an Agilent 6210 ESI-TOF instrument by Agilent Technologies with standard settings of 5 L/min, 4 kV and 15 psi for ESI-TOF. All other parameters have been optimized for each substance. IR spectra were measured on a Nicolet iS10 FTIR-ATR spectrometer by Thermo Scientific.

P,N-Rhenium(I) Carbonyl Complexes: In a dry box, the pyridylphosphinines were dissolved in dry toluene (0.5 mL) and added to pentacarbonyl rhenium(I) halide in a Young-NMR-tube. After heating to T = 80 °C for overnight, the bright yellow precipitate was filtered off and washed with a very small amount of toluene (≈ 0.2 mL) inside a dry box. Drying under vacuum gave the products as yellow solids.

2-(2-Pyridyl)-4,6-diphenylphosphinine-P,N-rhenium(I) Tricarbonyl Chloride (3): Pyridylphosphinine **1** (15 mg, 0.046 mmol) and [Re(CO)$_5$Cl] (17 mg, 0.047 mmol) gave the product (21 mg, 0.034 mmol, 74 %) as yellow crystals. ^1H NMR (401 MHz, CD_2Cl_2): δ = 7.42 (ddt, J = 7.1, 5.7, 1.3 Hz, 1 H), 7.46–7.66 (m, 6 H), 7.67–7.74 (m, 2 H), 7.83–7.91 (m, 2 H), 8.05–8.12 (m, 1 H), 8.30–8.36 (m, 1 H), 8.44 (dd, J = 19.6, 1.4 Hz, 1 H), 8.66 (dd, J = 15.6, 1.5 Hz, 1 H), 9.21–9.27 (m, 1 H) ppm; $^{13}C\{^1H\}$ NMR (101 MHz, CD_2Cl_2): δ = 121.2 (d, $J_{C,P}$ = 12.7 Hz), 126.8 (d, $J_{C,P}$ = 3.3 Hz), 128.3 (d, $J_{C,P}$ = 2.5 Hz), 129.0 (d, $J_{C,P}$ = 11.2 Hz), 129.3, 129.9, 130.0, 130.1, 132.9 (d, $J_{C,P}$ = 13.7 Hz), 138.5 (d, J = 12.3 Hz), 138.9 (d, J = 15.0 Hz), 140.3, 141.6 (d, J = 4.7 Hz), 143.3 (d, J = 24.1 Hz), 158.2 (d, $J_{C,P}$ = 2.9 Hz), 158.6 (d, $J_{C,P}$ = 23.0 Hz), 159.3 (d, $J_{C,P}$ = 21.3 Hz), 159.7 (d, $J_{C,P}$ = 16.0 Hz), 185.7 (d, $J_{C,P}$ = 11.6 Hz), 193.5 (d, $J_{C,P}$ = 52.4 Hz), 194.0 (d, $J_{C,P}$ = 32.1 Hz) ppm; $^{31}P\{^1H\}$ NMR (162 MHz, CD_2Cl_2): δ = 189.6 ppm. FT-IR (solid ATR): $\tilde{\nu}$ (CO) 2029, 1947, 1937, 1905 (sh), 1880 cm^{-1}.

2-(2-Pyridyl)-4,6-diphenylphosphinine-P,N-rhenium(I) Tricarbonyl Bromide (4): Pyridylphosphinine 1 (16 mg, 0.049 mmol) and [Re(CO)$_5$Br] (19 mg, 0.047 mmol) gave the product (21 mg, 0.032 mmol, 68 %) as yellow crystals. ^1H NMR (401 MHz, CD_2Cl_2):

δ = 7.40 (ddt, J = 7.3, 5.8, 1.3 Hz, 1 H), 7.46–7.65 (m, 6 H), 7.66–7.74 (m, 2 H), 7.83–7.91 (m, 2 H), 8.04–8.12 (m, 1 H), 8.29–8.36 (m, 1 H), 8.45 (dd, J = 19.9, 1.4 Hz, 1 H), 8.66 (dd, J = 15.7, 1.4 Hz, 1 H), 9.23–9.27 (m, 1 H) ppm; $^{13}C\{^1H\}$ NMR (101 MHz, CD_2Cl_2): δ = 121.3 (d, $J_{C,P}$ = 12.7 Hz), 126.6 (d, $J_{C,P}$ = 3.6 Hz), 128.3 (d, $J_{C,P}$ = 2.9 Hz), 129.1 (d, $J_{C,P}$ = 11.1 Hz), 129.2, 129.9, 129.9 (d, J = 2.0 Hz), 130.1, 132.8 (d, $J_{C,P}$ = 13.7 Hz), 138.5 (d, J = 12.2 Hz), 138.8 (d, J = 14.9 Hz), 140.2, 141.5 (d, J = 5.0 Hz), 143.2 (d, J = 24.1 Hz), 158.1 (d, $J_{C,P}$ = 2.9 Hz), 158.3 (d, $J_{C,P}$ = 3.2 Hz), 158.5 (d, $J_{C,P}$ = 22.5 Hz), 159.8 (d, $J_{C,P}$ = 15.9 Hz), 185.2 (d, $J_{C,P}$ = 11.5 Hz), 192.9 (d, $J_{C,P}$ = 40.9 Hz), 193.4 (d, $J_{C,P}$ = 40.5 Hz) ppm; $^{31}P\{^1H\}$ NMR (162 MHz, CD_2Cl_2): δ = 188.1 ppm. ESI-TOF (*m/z*): 669.9649 (calcd.: 669.9552 g/mol) $[M - CO + Na]^+$, 613.9751 (calcd.: 613.9659 g/mol) $[M - 3\ CO + Na]^+$, 568.0624 (calcd.: 568.0476 g/mol) $[M - CO - Br]^+$. FT-IR (solid ATR): $\tilde{\nu}$ (CO) 2026, 1935 (sh), 1899 cm^{-1}.

2-(2-Pyridyl)-4-(4-fluorophenyl)-6-phenylphosphinine-P,N-rhenium(I) Tricarbonyl Chloride (3-F): Pyridylphosphinine **1-F** (15 mg, 0.044 mmol) and $[Re(CO)_5Cl]$ (15 mg, 0.042 mmol) gave the product (19 mg, 0.029 mmol, 70 %) as yellow solid. ^1H NMR (401 MHz, CD_2Cl_2): δ = 7.25 (m, 2 H, $H^{19/21}$), 7.37–7.41 (m, 1 H, H^9), 7.54–7.58 (m, 1 H, H^{14}), 7.58–7.64 (m, 2 H, $H^{13/15}$), 7.64–7.70 (m, 2 H, $H^{18/22}$), 7.81–7.91 (m, 2 H, $H^{12/16}$), 8.01–8.12 (m, 1 H, H^8), 8.28–8.37 (m, 1 H, H^7), 8.38 (dd, J = 19.8, 1.4 Hz, 1 H, H^2 or H^4), 8.60 (dd, J = 15.7, 1.4 Hz, 1 H, H^2 or H^4), 9.20–9.29 (m, 1 H, H^{10}) ppm. ^{19}F NMR (376 MHz, CD_2Cl_2): δ = –113.7 (m_s) ppm; $^{31}P\{^1H\}$ NMR (162 MHz, CD_2Cl_2): δ = 188.1 ppm.

2-(2-Pyridyl)-4-(4-fluorophenyl)-6-phenylphosphinine-P,N-rhenium(I) Tricarbonyl Bromide (4-F): Pyridylphosphinine **1-F** (15 mg, 0.044 mmol) and $[Re(CO)_5Br]$ (17 mg, 0.042 mmol) gave the product (15 mg, 0.022 mmol, 52 %) as yellow solid. ^1H NMR (400 MHz, CD_2Cl_2): δ = 7.22 (m_s, 2 H, $H^{19/21}$), 7.34–7.39 (m, 1 H, H^9), 7.52–7.68 (m, 5 H, H^{14}, $H^{13/15}$, $H^{18/22}$), 7.81–7.85 (m, 2 H, $H^{12/16}$), 7.98–8.04 (m, 1 H, H^8), 8.29–8.32 (m, 1 H, H^7), 8.33 (dd, $^3J_{H-P}$ = 19.7, $^4J_{H,H}$ = 1.4 Hz, 1 H, H^2 or H^4), 8.53 (dd, $^3J_{H-P}$ = 15.7, $^4J_{H,H}$ = 1.4 Hz, 1 H, H^2 or H^4), 9.20 (ddd, J = 5.7, 1.7, 0.8 Hz, 1 H, H^{10}) ppm; $^{13}C\{^1H\}$ NMR (101 MHz, CD_2Cl_2): δ = 116.8 (d, $J_{C,F}$ = 21.8 Hz, $C^{19/21}$), 121.4 (d, $J_{C,P}$ = 12.7 Hz, C^7), 126.7 (d, $J_{C,P}$ = 3.5 Hz, C^9), 129.1 (d, $J_{C,P}$ = 11.1 Hz, $C^{12/16}$), 130.0 (d, $J_{C,P}$ = 2.1 Hz, C^{14}), 130.1 ($C^{13/15}$), 130.2 (dd, $J_{C,F}$ = 8.4, $J_{C,P}$ = 2.0 Hz, $C^{18/22}$), 132.6 (d, $J_{C,P}$ = 13.7 Hz, C^2 or C^4), 137.7 (dd, $J_{C,P}$ = 5.1, $J_{C,F}$ = 3.3 Hz, C^{17}), 138.3 (d, $J_{C,P}$ = 12.2 Hz, C^2 or C^4), 138.8 (d, $J_{C,P}$ = 15.0 Hz, C^{11}), 140.2 (C^8), 142.1 (d, $J_{C,P}$ = 24.3 Hz, C^3), 158.3 (d, $J_{C,P}$ = 23.9 Hz, C^1), 158.3 (d, $J_{C,P}$ = 3.2 Hz, C^{10}), 158.6 (d, $J_{C,P}$ = 22.4 Hz, C^5), 159.8 (d, $J_{C,P}$ = 16.2 Hz, C^6), 163.8 (d, $J_{C,F}$ = 247.6 Hz, C^{20}), 185.2 (d, $J_{C,P}$ = 11.5 Hz, CO), 192.9 (d, $J_{C,P}$ = 37.0 Hz, CO), 193.4 (d, $J_{C,P}$ = 43.7 Hz, CO) ppm. ^{19}F NMR (376 MHz, CD_2Cl_2): δ = –113.7 (m_s) ppm; $^{31}P\{^1H\}$ NMR (162 MHz, CD_2Cl_2): δ = 189.9 ppm.

NN-Rhenium(I) Carbonyl Complexes: Bipyridines were dissolved in DCM (0.5 mL) and added to pentacarbonyl rhenium(I) halide in an NMR-tube. After heating to T = 40 °C for t = 4 h, the bright yellow precipitate was filtered off and washed with a very small amount of cold DCM (≈ 0.2 mL). Drying under vacuum gave the products as yellow solids.

2-(2-Pyridyl)-4,6-diphenylpyridine-*N*,*N*-rhenium(I) Tricarbonyl Chloride (5): Bipyridine **2** (36 mg, 0.117 mmol) and $[Re(CO)_5Cl]$ (43 mg, 0.119 mmol) gave the product (58 mg, 0.095 mmol, 81 %) as yellow crystals. Crystals suitable for X-ray diffraction were obtained from a NMR solution in $[D_6]$DMSO. ^1H NMR (400 MHz, $[D_6]$DMSO): δ = 7.55–7.75 (m, broad, 8 H, $H^{12/16}$, $H^{13/15}$, H^{14}, $H^{19/21}$, H^{20}), 7.75–7.81 (m, 1 H, H^9), 8.10 (d, J = 2.1 Hz, 1 H, H^2), 8.17–8.24 (m, 2 H, $H^{18/22}$), 8.35–8.42 (m, 1 H, H^8), 8.97 (d, J = 1.8 Hz, 1 H, H^4), 8.95–8.98 (m, 1 H, H^7), 9.02–9.05 (m, 1 H, H^{10}) ppm; $^{13}C\{^1H\}$ NMR (101 MHz, $[D_2]$DCM): δ = 120.4 (C^4), 124.9 (C^2), 125.8 (C^7), 127.9 (C^9), 128.2 ($C^{18/22}$), 129.6 ($C^{12/16}$ or $C^{13/15}$), 129.8 ($C^{19/21}$), 130.4 (C^{14}), 131.3 (C^{20}), 135.2 (C^{17}), 140.4 (C^8), 142.1 (C^{11}), 150.9 (C^3), 153.1 (C^{10}), 156.5 (C^5 or C^6), 157.3 (C^5 or C^6), 163.7 (C^1), 191.6 (CO), 194.0 (CO), 198.0 (CO) ppm. ESI-TOF (*m/z*): 653.0046 (calcd.: 653.0044 g/mol) $[M + K]^+$, 637.0306 (calcd.: 637.0305 g/mol) $[M + Na]^+$, 579.0727 (calcd.: 579.0719 g/mol) $[M - Cl]^+$. FT-IR (solid ATR): $\tilde{\nu}$ (CO) 2017, 1938, 1907, 1864 cm^{-1}.

2-(2-Pyridyl)-4,6-diphenylpyridine-*N*,*N*-rhenium(I) Tricarbonyl Bromide (6): Bipyridine **2** (36 mg, 0.117 mmol) and $[Re(CO)_5Br]$ (48 mg, 0.118 mmol) gave the product (54 mg, 0.082 mmol, 70 %) as yellow crystals. ^1H NMR (400 MHz, $[D_6]$DMSO): δ = 7.54–7.73 (m, broad, 8 H, $H^{12/16}$, $H^{13/15}$, H^{14}, $H^{19/21}$, H^{20}), 7.73–7.78 (m, 1 H, H^9), 8.04 (d, J = 1.9 Hz, 1 H, H^2), 8.12–8.16 (m, 2 H, $H^{18/22}$), 8.30–8.36 (m, 1 H, H^8), 8.98 (d, J = 1.9 Hz, 1 H, H^4), 9.00–9.04 (m, 1 H, H^7), 9.04–9.07 (m, 1 H, H^{10}) ppm; $^{13}C\{^1H\}$ NMR (101 MHz, $[D_6]$DMSO): δ = 120.4 (C^4), 124.9 (C^2), 125.7 (C^7), 127.8 (C^9), 128.1 ($C^{18/22}$), 129.4 ($C^{12/16}$ or $C^{13/15}$), 129.8 ($C^{19/21}$), 130.3 (C^{14}), 131.3 (C^{20}), 135.1 (C^{17}), 140.3 (C^8), 142.2 (C^{11}), 150.8 (C^3), 153.2 (C^{10}), 157.0 (C^5 or C^6), 157.3 (C^5 or C^6), 163.9 (C^1), 190.9 (CO), 193.5 (CO), 197.7 (CO) ppm. ESI-TOF (*m/z*): 680.9794 (calcd.: 680.9800 g/mol) $[M + Na]^+$, 607.0710 (calcd.: 607.0668 g/mol) $[M - Br + CO]^+$, 579.0729 (calcd.: 579.0719 g/mol) $[M - Br]^+$, 551.0776 (calcd.: 551.0769 g/mol) $[M - Br - CO]^+$, 523.0867 (calcd.: 523.0820 g/mol) $[M - Br - 2\ CO]^+$. FT-IR (solid ATR): $\tilde{\nu}$ (CO) 2018, 1940, 1911, 1867 cm^{-1}.

2-(2-Pyridyl)-4-(4-fluorophenyl)-6-phenylpyridine-*N*,*N*-rhenium(I) Tricarbonyl Chloride (5-F): Bipyridine **2-F** (32 mg, 0.098 mmol) and $[Re(CO)_5Cl]$ (36 mg, 0.100 mmol) gave the product (51 mg, 0.081 mmol, 82 %) as yellow crystals. Crystals suitable for X-ray diffraction were obtained from cooling down a DCM solution. ^1H NMR (400 MHz, $[D_6]$DMSO): δ = 7.42–7.49 (m, 2 H, $H^{19/21}$), 7.54–7.75 (m, broad, 5 H, $H^{12/16}$, $H^{13/15}$, H^{14}), 7.75–7.80 (m, 1 H, H^9), 8.09 (d, J = 1.9 Hz, 1 H, H^2), 8.26–7.32 (m, 2 H, $H^{18/22}$), 8.33–8.41 (m, 1 H, H^8), 9.02 (d, J = 1.9 Hz, 1 H, H^4), 9.04–9.10 (m, 2 H, H^{10}, H^7) ppm; $^{13}C\{^1H\}$ NMR (101 MHz, $[D_6]$DMSO): δ = 116.3 (d, $^2J_{C,F}$ = 21.7 Hz, $C^{19/21}$), 120.0 (d, C^4), 124.5 (C^2), 125.5 (C^7), 127.5 (C^9), 129.3 ($C^{12/16}$ or $C^{13/15}$), 129.9 (C^{14}), 130.5 (d, $^3J_{C,F}$ = 8.8 Hz, $C^{18/22}$), 131.3 (C^{17}), 139.9 (C^8), 141.7 (C^{11}), 149.3 (C^3), 152.7 (C^{10}), 156.6 (C^5 or C^6), 156.9 (C^5 or C^6), 162.6 (C^1), 163.9 (d, $^1J_{C,F}$ = 249.4 Hz, C^{20}), 191.2 (CO), 193.7 (CO), 197.7 (CO) ppm. ^{19}F NMR (376 MHz, [D]MSO): δ = –110.0 (m_s) ppm. ESI-TOF (*m/z*): 670.9937 (calcd.: 670.9950 g/mol) $[M + K]^+$, 655.0201 (calcd.: 655.0210 g/mol) $[M + Na]^+$, 625.0592 (calcd.: 625.0574 g/mol) $[M - Cl + CO]^+$, 597.0631 (calcd.: 597.0624 g/mol) $[M - Cl]^+$, 569.0657 (calcd.: 569.0675 g/mol) $[M - Cl - CO]^+$, 541.0718 (calcd.: 541.0726 g/mol) $[M - Cl - 2\ CO]^+$. FT-IR (solid ATR): $\tilde{\nu}$ (CO) 2014, 1914, 1871, 1852 (sh) cm^{-1}.

2-(2-Pyridyl)-4-(4-fluorophenyl)-6-phenylpyridine-*N*,*N*-rhenium(I) Tricarbonyl Bromide (6-F): Bipyridine **2-F** (33 mg, 0.101 mmol) and $[Re(CO)_5Br]$ (41 mg, 0.1009 mmol) gave the product (46 mg, 0.068 mmol, 67 %) as yellow crystals. Crystals suitable for X-ray diffraction were obtained from a reaction mixture in DCM. ^1H NMR (400 MHz, $[D_6]$DMSO): δ = 7.42–7.49 (m, 2 H, $H^{19/21}$), 7.55–7.75 (m, broad, 5 H, $H^{12/16}$, $H^{13/15}$, H^{14}), 7.77 (ddd, J = 7.5, 5.5, 1.2 Hz, 1 H, H^9), 8.10 (d, J = 1.9 Hz, 1 H, H^2), 8.27–7.34 (m, 2 H, $H^{18/22}$), 8.34–8.41 (m, 1 H, H^8), 9.04 (d, J = 1.9 Hz, 1 H, H^4), 9.06–9.12 (m, 2 H, H^{10}, H^7) ppm; $^{13}C\{^1H\}$ NMR (101 MHz, $[D_6]$DMSO): δ = 116.3 (d, $^2J_{C,F}$ = 21.7 Hz, $C^{19/21}$), 120.1 (d, C^4), 124.5 (C^2), 125.5 (C^7), 127.5 (C^9), 129.2 ($C^{12/16}$ or $C^{13/15}$), 129.9 (C^{14}), 130.6 (d, $^3J_{C,F}$ = 8.8 Hz, $C^{18/22}$), 131.3 (d, $^4J_{C,F}$ = 3.0 Hz, C^{17}), 139.9 (C^8), 141.9 (C^{11}), 149.2 (C^3), 152.9 (C^{10}), 156.7 (C^5 or C^6), 156.9 (C^5 or C^6), 163.7 (C^1), 163.9 (d, $^1J_{C,F}$ = 249.5 Hz, C^{20}), 190.6 (CO), 193.7 (CO), 197.4 (CO) ppm. ^{19}F NMR (376 MHz, [D]MSO): δ = –109.9 (tt, $^3J_{F,H}$ = 8.8, $^4J_{F,H}$ = 5.3 Hz) ppm.

ESI-TOF (*m/z*): 670.9937 (calcd.: 670.9950 g/mol) $[M + K]^+$, 698.9672 (calcd.: 698.9705 g/mol) $[M + Na]^+$, 625.0739 (calcd.: 625.0574 g/mol) $[M - Br + CO]^+$, 597.0660 (calcd.: 597.0624 g/mol) $[M - Br]^+$, 569.0649 (calcd.: 569.0675 g/mol) $[M - Br - CO]^+$, 541.0724 (calcd.: 541.0726 g/mol) $[M - Br - 2\ CO]^+$. FT-IR (solid ATR): $\tilde{\nu}$ (CO) 2017, 1958 (sh), 1914, 1874 cm^{-1}.

Reactivity of [(P^N)Re(CO)$_3$Br] (4) Towards Water: In a J. Young NMR tube the pyridylphosphinine rhenium(I) complex **4** (0.027 mmol) was dissolved in deuterated DCM (0.45 mL) and degassed water (1 µL, 1 mg, 0.055 mmol, 2 equiv.) was added. $^{31}P\{^1H\}$ NMR (162 MHz, CD_2Cl_2): δ = 72.9, 81.2, 95.2, 107.2 ppm.

Crystallographic Data for 4: $C_{25}H_{16}BrNO_3PRe$ + disordered CH_2Cl_2, Fw = 675.47,[*] yellow block, 0.42 × 0.36 × 0.18 mm^3, triclinic, $P\bar{1}$ (no. 2), a = 7.04724(17), b = 11.6974(4), c = 15.2629(3) Å, α = 89.723(1), β = 84.650(1), γ = 82.676(2)°, V = 1242.45(6) $Å^3$, Z = 2, D_x = 1.806 g/cm^3,[*] μ = 6.59 mm^{-1}.[*] The diffraction experiment was performed on a Nonius KappaCCD diffractometer with rotating anode and graphite monochromator (λ = 0.71073 Å) at a temperature of 150(2) K up to a resolution of $(\sin\theta/\lambda)_{max}$ = 0.65 $Å^{-1}$. The Eval14 software[17] was used for the intensity integration. An analytical absorption correction and scaling was performed with SADABS[18] (correction range 0.06–0.35). A total of 36216 reflections were measured, 5704 reflections were unique (R_{int} = 0.024), of which 5309 were observed [$I > 2\sigma(I)$]. The structure was solved with Direct Methods using SHELXS-97.[19] Least-squares refinement was performed with SHELXL-2018[20] against F^2 of all reflections. The crystal structure contains a large void on an inversion center (162 $Å^3$/unit cell) filled with a severely disordered CH_2Cl_2 molecule. Its contribution to the structure factors was secured by back-Fourier transformation with the SQUEEZE algorithm.[21] This resulted in 44 electrons/unit cell. Non-hydrogen atoms were refined freely with anisotropic displacement parameters. Hydrogen atoms were introduced in calculated positions and refined with a riding model. 289 Parameters were refined with no restraints. $R1/wR2$ [$I > 2\sigma(I)$]: 0.0135 / 0.0285. $R1/wR2$ [all refl.]: 0.0166/0.0291. S = 1.057. Residual electron density between –0.35 and 0.50 e/$Å^3$. Geometry calculations and checking for higher symmetry was performed with the PLATON program.[22] [*] Derived values do not contain the contribution of the disordered dichloromethane.

Crystallographic Data for 5: $C_{25}H_{16}BrN_2O_3Re$, Fw = 658.51, yellow block, 0.24 × 0.21 × 0.21 mm^3, monoclinic, $P2_1/c$ (no. 14), a = 11.79475(19), b = 11.6823(2), c = 16.0977(3) Å, β = 102.655(1)°, V = 2164.21(7) $Å^3$, Z = 4, D_x = 2.021 g/cm^3, μ = 7.49 mm^{-1}. The diffraction experiment was performed on a Nonius KappaCCD diffractometer with rotating anode and graphite monochromator (λ = 0.71073 Å) at a temperature of 150(2) K up to a resolution of $(\sin\theta/\lambda)_{max}$ = 0.65 $Å^{-1}$. The Eval15 software[23] was used for the intensity integration. A multiscan correction and scaling was performed with SADABS[602] (correction range 0.35–0.43). A total of 52508 reflections were measured, 4974 reflections were unique (R_{int} = 0.024), of which 4585 were observed [$I > 2\sigma(I)$]. The structure was solved with automated Patterson methods using DIRDIF-99.[24] Least-squares refinement was performed with SHELXL-2018[20] against F^2 of all reflections. Non-hydrogen atoms were refined freely with anisotropic displacement parameters. Hydrogen atoms were located in difference Fourier maps and refined with a riding model. 289 Parameters were refined with no restraints. $R1/wR2$ [$I > 2\sigma(I)$]: 0.0141/0.0311. $R1/wR2$ [all refl.]: 0.0173/0.0321. S = 1.075. Residual electron density between –0.49 and 0.44 e/$Å^3$. Geometry calculations and checking for higher symmetry was performed with the PLATON program.[22]

Crystallographic Data for 5-F: $C_{25}H_{15}FClN_2O_3Re$, CH_2Cl_2, Fw = 716.98, 0.75 × 0.02 × 0.02 mm^3, yellow needle, monoclinic, $P2_1/c$, a = 7.4816(4), b = 19.8766(10), c = 17.1967(9) Å, β = 99.301(2)°, V = 2523.7(2) $Å^3$, Z = 4, D_x = 1.887 g cm^{-3}, μ = 5.17 mm^{-1}. 97039 reflections were measured by using a Bruker D8-Venture Photon area detector (Mo-K_α radiation, λ = 0.71073 Å) up to a resolution of $(\sin\theta/\lambda)_{max}$ = 0.63 $Å^{-1}$ at a temperature of 100 K. The reflections were corrected for absorption and scaled on the basis of multiple measured reflections by using the SADABS program (0.60–0.75 correction range).[25] 5002 reflections were unique (R_{int} = 0.032). Using Olex,[26] the structures were solved with SHELXS-97 by using direct methods and refined with SHELXL-97 on F^2 for all reflections.[20] The structure is refined as an 2-component twin.[25] Non-hydrogen atoms were refined by using anisotropic displacement parameters. The positions of the hydrogen atoms were calculated for idealized positions. 330 parameters were refined without restraints. R_1 = 0.025 for 5002 reflections with $I > 2\sigma(I)$ and wR_2 = 0.057 for 5236 reflections, S = 1.127, residual electron density was between –2.37 and 0.62 e $Å^{-3}$. Geometry calculations and checks for higher symmetry were performed with the PLATON program.[22]

Crystallographic Data for 6-F: $C_{25}H_{15}FBrN_2O_3Re$, CD_2Cl_2, Fw = 763.43, 0.35 × 0.05 × 0.03 mm^3, yellow needle, monoclinic, $P2_1/c$, a = 7.5465(2), b = 20.0061(5), c = 17.3842(5) Å, β = 99.904(1)°, V = 2585.48(12) $Å^3$, Z = 4, D_x = 1.961 g cm^{-3}, μ = 6.49 mm^{-1}. 20982 reflections were measured by using a Bruker D8-Venture Photon area detector (Mo-K_α radiation, λ = 0.71073 Å) up to a resolution of $(\sin\theta/\lambda)_{max}$ = 0.63 $Å^{-1}$ at a temperature of 100 K. The reflections were corrected for absorption and scaled on the basis of multiple measured reflections by using the SADABS program (0.60–0.75 correction range).[25] 4858 reflections were unique (R_{int} = 0.020). Using Olex,[26] the structures were solved with SHELXS-97 by using direct methods and refined with SHELXL-97 on F^2 for all reflections.[20] Non-hydrogen atoms were refined by using anisotropic displacement parameters. The positions of the hydrogen atoms were calculated for idealized positions. 343 parameters were refined without restraints. R_1 = 0.017 for 4858 reflections with $I > 2\sigma(I)$ and wR_2 = 0.051 for 5265 reflections, S = 1.226, residual electron density was between –0.89 and 0.67 e $Å^{-3}$. Geometry calculations and checks for higher symmetry were performed with the PLATON program.[22]

CCDC 1869344 (for **4**), 1869345 (for **6**), 1868407 (for **5-F**), and 1868408 (for **6-F**) contain the supplementary crystallographic data for this paper. These data can be obtained free of charge from The Cambridge Crystallographic Data Centre.

Acknowledgments

A. L., M. W., and C. M. thank the Deutsche Forschungsgemeinschaft (DFG) and Freie Universität Berlin for financial support.

Keywords: Phosphorus · Heterocycles · P,N ligands · Coordination chemistry · Structure elucidation

[1] See for example: a) D. W. Thompson, A. Ito, T. J. Meyer, *Pure Appl. Chem.* **2013**, *85*, 1257; b) A. Adeloye, P. Ajibade, *Molecules* **2014**, *19*, 12421; c) F. Puntoriero, S. Serroni, F. Nastasi, S. Campagna in *Electrochemistry of Functional Supramolecular Systems*, John Wiley & Sons, Inc.: Hoboken, NJ, USA, **2010**, pp. 121–143; d) F. Teplý, *Collect. Czechoslov. Chem. Commun.* **2011**, *76*, 859..

[2] a) G. Märkl, *Angew. Chem. Int. Ed. Engl.* **1966**, *5*, 846; *Angew. Chem.* **1966**, *78*, 907; b) A. J. Ashe, *J. Am. Chem. Soc.* **1971**, *93*, 3293.

[3] a) J.-M. Alcaraz, A. Brèque, F. Mathey, *Tetrahedron Lett.* **1982**, *23*, 1565–1568; b) P. Le Floch, D. Charmichael, L. Ricard, F. Mathey, *J. Am. Chem. Soc.* **1993**, *115*, 10665–10670.

[4] a) B. Schmid, L. M. Venanzi, A. Albinati, F. Mathey, *Inorg. Chem.* **1991**, *30*, 4693–4699; B. Schmid, L. M. Venanzi, T. Gerfin, F. Gramlich, F. Mathey, *Inorg. Chem.* **1992**, *31*, 5117–5122.
[5] C. Müller, D. Wasserberg, J. J. M. Weemers, E. A. Pidko, S. Hoffmann, M. Lutz, A. L. Spek, S. C. J. Meskers, R. A. Janssen, R. A. van Santen, D. Vogt, *Chem. Eur. J.* **2007**, *13*, 4548.
[6] a) A. Campos Carrasco, E. A. Pidko, A. M. Masdeu-Bultó, M. Lutz, A. L. Spek, D. Vogt, C. Müller, *New J. Chem.* **2010**, *34*, 1547–1550; b) I. de Krom, L. E. E. Broeckx, M. Lutz, C. Müller, *Chem. Eur. J.* **2013**, *19*, 3676–3684.
[7] a) C. Müller, D. Vogt, *C. R. Chim.* **2010**, *13*, 1127–1143; b) A. Campos-Carrasco, L. E. E. Broeckx, J. J. M. Weemers, E. A. Pidko, M. Lutz, A. M. Masdeu-Bultó, D. Vogt, C. Müller, *Chem. Eur. J.* **2011**, *17*, 2510–2517; c) C. Müller, L. E. E. Broeckx, I. de Krom, J. J. M. Weemers, *Eur. J. Inorg. Chem.* **2013**, 187; d) I. de Krom, E. A. Pidko, M. Lutz, C. Müller, *Chem. Eur. J.* **2013**, *19*, 7523–7531; e) M. Bruce, G. Meissner, M. Weber, J. Wiecko, C. Müller, *Eur. J. Inorg. Chem.* **2014**, 1719–1726; f) C. Müller, J. A. W. Sklorz, I. de Krom, A. Loibl, M. Habicht, M. Bruce, G. Pfeifer, J. Wiecko, *Chem. Lett.* **2014**, *43*, 1390–1404; g) G. Pfeifer, P. Ribagnac, X.-F. Le Goff, J. Wiecko, N. Mézailles, C. Müller, *Eur. J. Inorg. Chem.* **2015**, 240–249; h) I. de Krom, M. Lutz, C. Müller, *Dalton Trans.* **2015**, *44*, 10304–10314.
[8] M. Hollering, R. O. Reithmeier, S. Meister, E. Herdtweck, F. E. Kühn, B. Rieger, *RSC Adv.* **2016**, *6*, 14134.
[9] See for example: a) J. Hawecker, J. M. Lehn, R. Ziessel, *Helv. Chim. Acta* **1986**, *69*, 1990; b) J. Hawecker, J.-M. Lehn, R. Ziessel, *J. Chem. Soc., Chem. Commun.* **1983**, *9*, 536; c) J. Hawecker, J.-M. Lehn, R. Ziessel, *J. Chem. Soc., Chem. Commun.* **1984**, *6*, 328; d) R. Reithmeier, C. Bruckmeier, B. Rieger, *Catalysts* **2012**, *2*, 544.
[10] A. Loibl, I. de Krom, E. A. Pidko, M. Weber, J. Wiecko, C. Müller, *Chem. Commun.* **2014**, *50*, 8842–8844.
[11] A. Loibl, W. Oschmann, M. Vogler, E. A. Pidko, M. Weber, J. Wiecko, C. Müller, *Dalton Trans.* **2018**, *47*, 9355–9366.
[12] See for example: a) M. Wrighton, D. L. Morse, *J. Am. Chem. Soc.* **1974**, *96*, 998; b) L. A. Worl, R. Duesing, P. Chen, L. Della Ciana, T. J. Meyer, *J. Chem. Soc., Dalton Trans.* **1991**, *0*, 849–858.
[13] S. Sato, T. Morimoto, O. Ishitani, *Inorg. Chem.* **2007**, *46*, 9051.
[14] M. H. Chisholm, J. C. Huffman, I. P. Rothwell, P. G. Bradley, N. Kress, W. H. Woodruff, *J. Am. Chem. Soc.* **1981**, *103*, 4945.
[15] a) N. Mézailles, F. Mathey, P. Le Floch, *Prog. Inorg. Chem.* **2001**, *49*, 455; b) P. Le Floch, F. Mathey, *Coord. Chem. Rev.* **1998**, *178–180*, 771; c) P. Le Floch, *Coord. Chem. Rev.* **2006**, *250*, 627.
[16] a) J. Waluk, H.-P. Klein, A. J. Ashe III, J. Michl, *Organometallics* **1989**, *8*, 2804; b) E. F. DiMauro, M. C. Kozlowski, *J. Chem. Soc., Perkin Trans. 1* **2002**, 439; c) L. Nyulászi, *Chem. Rev.* **2001**, *101*, 1229–1246.
[17] A. J. M. Duisenberg, L. M. J. Kroon-Batenburg, A. M. M. Schreurs, *J. Appl. Crystallogr.* **2003**, *36*, 220–229.
[18] G. M. Sheldrick (**2008**). SADABS. Universität Göttingen, Germany.
[19] G. M. Sheldrick, *Acta Crystallogr., Sect. A* **2008**, *64*, 112–122.
[20] G. M. Sheldrick, *Acta Crystallogr., Sect. C* **2015**, *71*, 3–8.
[21] A. L. Spek, *Acta Crystallogr., Sect. C* **2015**, *71*, 9–18.
[22] A. L. Spek, *Acta Crystallogr., Sect. D* **2009**, *65*, 148–155.
[23] A. M. M. Schreurs, X. Xian, L. M. J. Kroon-Batenburg, *J. Appl. Crystallogr.* **2010**, *43*, 70–82.
[24] P. T. Beurskens, G. Beurskens, R. de Gelder, S. Garcia-Granda, R. O. Gould, and J. M. M. Smits (**2008**). The DIRDIF2008 program system, Crystallography Laboratory, University of Nijmegen, The Netherlands.
[25] Bruker (**2013**). *APEX2*, *SAINT* and *SADABS*. Bruker AXS Inc., Madison, Wisconsin, USA.
[26] *Olex2*: a complete structure solution, refinement and analysis program. O. V. Dolomanov, L. J. Bourhis, R. J. Gildea, J. A. Howard, H. Puschmann, *J. Appl. Crystallogr.* **2009**, *42*, 339–341.

Received: October 9, 2018